



# High Mass-Loading Sulfur-Composite Cathode for Lithium-Sulfur Batteries

Nurzhan Baikalov<sup>1,2</sup>, Nurassyl Serik<sup>2</sup>, Sandugash Kalybekkyzy<sup>1,2</sup>, Indira Kurmanbayeva<sup>1,3</sup>, Zhumabay Bakenov<sup>1,2,3</sup> and Almagul Mentbayeva<sup>1,2\*</sup>

<sup>1</sup> National Laboratory Astana, Nazarbayev University, Nur-Sultan, Kazakhstan, <sup>2</sup> School of Engineering and Digital Sciences, Nazarbayev University, Nur-Sultan, Kazakhstan, <sup>3</sup> Institute of Batteries LLC, Nur-Sultan, Kazakhstan

This research aimed to increase the mass loading of sulfur in the composite electrode in order to increase the energy density of the lithium-sulfur (Li-S) cell. This requires designing the electrode with the use of conductive agents to maintain the conductivity of the sulfur composite. Therefore, the composite of sulfur with polyacrylonitrile (PAN) and carbon nanotubes (CNT) was synthesized by heating. Following that, the mass loading of sulfur was increased by using several layers of carbon fiber paper (CFP) with a large free space as a three-dimensional current collector. As a result of the heat treatment and formation of covalent bonding between pyrolyzed PAN and sulfur, uniform distribution and enhanced conductivity were achieved, while CNT maintained structural integrity, acting as an interwoven network. Due to these advantages, the mass loading of sulfur was increased up to 5 mg cm<sup>-2</sup> while maintaining a high initial specific capacity of 1400 mAh g<sup>-1</sup> and stable cyclability.

**Keywords:** lithium-sulfur battery, composite cathode, 3D current collector, carbon fiber paper, mass loading

## OPEN ACCESS

### Edited by:

Yan-Bing He,  
Tsinghua University, China

### Reviewed by:

Huiqi Wang,  
North University of China, China  
Guangmin Zhou,  
Tsinghua University, China  
Bin Wang,  
China Academy of Engineering  
Physics, China

### \*Correspondence:

Almagul Mentbayeva  
almagul.mentbayeva@nu.edu.kz

### Specialty section:

This article was submitted to  
Electrochemical Energy Conversion  
and Storage,  
a section of the journal  
Frontiers in Energy Research

**Received:** 25 May 2020

**Accepted:** 03 August 2020

**Published:** 06 October 2020

### Citation:

Baikalov N, Serik N,  
Kalybekkyzy S, Kurmanbayeva I,  
Bakenov Z and Mentbayeva A (2020)  
High Mass-Loading Sulfur-Composite  
Cathode for Lithium-Sulfur Batteries.  
Front. Energy Res. 8:207.  
doi: 10.3389/fenrg.2020.00207

## INTRODUCTION

The development of electric vehicles and portable devices require high power and high energy density batteries. In this regard, among the existing energy storage systems, lithium-ion batteries (LIBs) play a key role since they offer the highest power density among all known secondary batteries. Also, LIBs have important advantages such as good rate capability and long cycle life. However, the energy and power densities of conventional LIBs are reaching limited theoretical values and cannot fulfill the requirements of the new generation of portable devices and electric vehicles (Ye et al., 2016). It is mainly due to the low theoretical capacity of currently available intercalated cathode materials such as LiCoO<sub>2</sub> and LiNi<sub>1/3</sub>Co<sub>1/3</sub>Mn<sub>1/3</sub>O<sub>2</sub> (about 150 mAh g<sup>-1</sup> and 188 mAh g<sup>-1</sup>, respectively) (Shin et al., 2011; Li M. et al., 2017). In addition, these transition metals are expensive and toxic. Therefore, alternative cathodes offering higher capacity with inexpensive, abundant, and environmentally friendly resources have to be developed (Nie et al., 2015).

A promising replacement for intercalated cathode materials is sulfur, since it has a high theoretical specific capacity and a high gravimetric energy density (1672 mAh g<sup>-1</sup> and 2600 Wh kg<sup>-1</sup>, respectively) (Shin et al., 2011). Moreover sulfur has several advantages associated with low cost, environmental friendliness, and abundant resources (Hara et al., 2015; Zeng et al., 2015). However, lithium-sulfur (Li-S) battery implementation is hindered by several difficulties related to the low conductivity of sulfur and the complexity of the redox process (Li M. et al., 2017). Firstly, sulfur has low ionic and electrical conductivity (5 × 10<sup>-30</sup> S cm<sup>-1</sup>) (Nie et al., 2015).

Another problem is the formation of polysulfides, intermediate products of sulfur reduction and its dissolution in the electrolytes (Yang et al., 2014; Li et al., 2018). Polysulfides shuttle back and forth during the redox reaction leading to the loss of the active material, thus generating free space in the cathode and increasing viscosity of the liquid electrolyte (Ould Ely et al., 2018). Then polysulfides precipitate at the anode side in the form of low order lithium sulfides ( $\text{Li}_2\text{S}_2$  and  $\text{Li}_2\text{S}$ ) (Kalybekkyzy et al., 2019). The reduction to  $\text{Li}_2\text{S}$  causes large volume expansion, which leads to non-linear discharge and charge of the cell and limited cyclability (Ma and Xu, 2018; Rajkumar et al., 2019). All these issues generate rapid capacity fade, low coulombic efficiency, and low power capability.

Various strategies were addressed in order to solve the aforementioned problems such as the fabrication of composite materials using conductive polymers like polypyrrole (Zhang et al., 2012), polyaniline (Yuan et al., 2009), polyacrylonitrile (PAN) (Wang et al., 2003), carbon additives such as multi-walled carbon nanotubes (MWCNTs) (Zhang Y. et al., 2014), graphene (Li et al., 2019), graphene oxide (Peng et al., 2018), and porous carbon (Li T. et al., 2017). These efforts are generally aimed at to improve the electrical conductivity of sulfur and limit polysulfides dissolution into the electrolyte (Bakenov et al., 2017). The group of Wang was among the first to work on the fabrication of molecular-level sulfur composites, where they synthesized a sulfur-dehydrogenated polyacrylonitrile (S/DPAN) composite by heating the mixture of sulfur and PAN at 280–300°C (Wang et al., 2003). The fixing of sulfur by a conductive polymer skeleton improved cyclability and capacity of the Li-S battery (Wang et al., 2003). Covalent bonding between sulfur and cyclized conductive DPAN in some degree maintains polysulfide dissolution (Zhang et al., 2012). Also, it was investigated that the addition of conductive hosts such as graphene (Yin et al., 2012), porous carbon (Li T. et al., 2017), and carbon nanotubes (Guo et al., 2011) to the mixture of S/DPAN further improves the electrochemical performance of the electrode (Peng et al., 2017b). However, the addition of inactive conductive materials into the composite decreases the sulfur content, which in turn affects the energy density of Li-S batteries (Zhao et al., 2015).

An increase in the amount of inactive materials (polymer, carbon) significantly reduces the weight content of sulfur, resulting in low mass loading. Low mass loading of sulfur notably decreases the energy density (Peng et al., 2017a). Moreover, conventional thin 2D metallic foil (Al) current collectors are incapable of providing high mass loading of sulfur ( $\leq 2 \text{ mg cm}^{-2}$ ) (Cheng et al., 2016). Therefore, alternative current collectors which enable high mass loading of sulfur need to be developed. There have been numerous attempts to increase mass loading and the areal capacity of sulfur using three-dimensional (3D) structures on metallic current collectors (Yu et al., 2018), freestanding carbon materials [including carbon nanotubes (Ye et al., 2016), doped carbon nanofibers (Song et al., 2017), 3D graphene composite foams (Lu et al., 2014)], structural confinement using hollow carbon nanofibers (Chung et al., 2016; Chung and Manthiram, 2018), and electro-spun 3D carbon nanofibers (Kalybekkyzy et al., 2020). These approaches are mainly based on the confinement of sulfur in conductive

hosts, which enables them to limit polysulfide dissolution and thus, increases the lifetime of batteries. Among these candidates 3D carbon current collectors such as carbon fiber paper (CFP) attracts a lot of attention due to its good electrical conductivity, high mechanical and chemical stability, low density, and low cost (Yuan et al., 2009; Suktha et al., 2015).

Herein we report a simple and efficient preparation method for high mass loading sulfur composite cathodes by designing micro- and nano-level 3D carbon networks. It was achieved through synthesis of S/DPAN/CNT composite cathodes by heat treatment in an argon atmosphere, where covalent bonding between pyrolyzed PAN and sulfur diminished polysulfide dissolution, while CNT maintained structural integrity, acting as a nanoscale interwoven network and ensured electron transfer within and between the S/DPAN granules (Mentbayeva et al., 2016). Then S/DPAN/CNT was impregnated into the voids of the commercial CFP, which in its turn was used in several layers to provide bulk electron conductivity at the macro-level. As a result, mass loading of sulfur was increased up to  $5 \text{ mg cm}^{-2}$ .

## EXPERIMENTAL PART

### Chemicals

Sulfur (98%, GOST 127.1, Tengizchevroil, Kazakhstan), polyacrylonitrile (average  $M_r = 150,000$ , J&K Scientific), multi-walled carbon nanotubes (CNT, >95%, OD: 10–20 nm, US Research Nanomaterials, Inc.), N-methyl-pyrrolidone (NMP) (>99%, Sigma-Aldrich), and polyvinylidene fluoride (PVdF, 100%, Arkema, MTI Corp.).

### Preparation of S/DPAN/CNT Composite Cathode

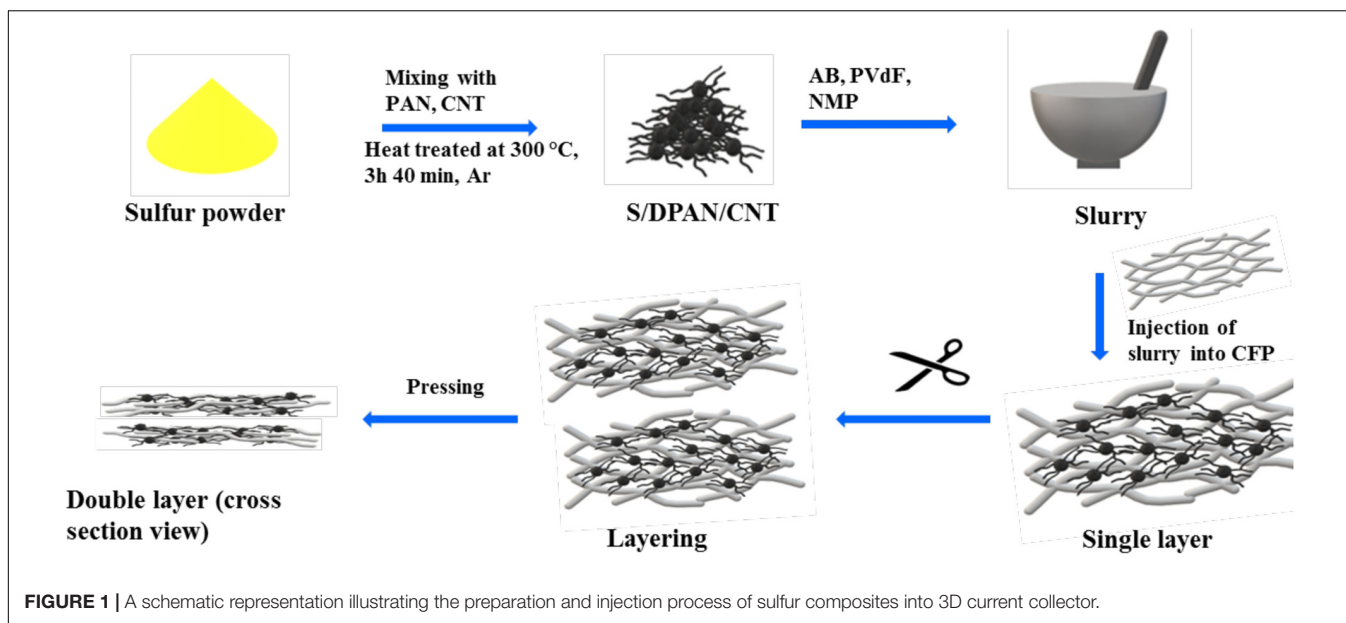
Sulfur was manually ground and mixed with PAN at the mass ratio of 4:1 with the addition of different amounts of CNT (1–4 wt% of total mass) as illustrated in **Figure 1**. After that, the mixture was heated in a tube furnace at 300°C with different durations of time (3 h and 40 min) in the argon atmosphere to form the S/DPAN/CNT composite.

### Physical-Chemical Characterization

X-ray diffraction (XRD, Rigaku SmartLab) was used in the structure analysis. The morphology of the samples were analyzed using scanning electron microscopy (F&SEM-EDS Auriga, Crossbeam 540), Raman spectroscopy (HORIBA Scientific, France), and Fourier transform infrared spectroscopy (Nicolet iS10 FT-IR Spectrometer); the sulfur content of composites was analyzed using elemental chemical analysis (CHNS, Vario Micro Cube, Elementar).

### Electrochemical Characterization

The electrochemical performance was analyzed using a CR2032 coin type cell configuration assembled in an argon filled glovebox (MasterLab, MBraun). Lithium metal disks were used as an anode, a porous polypropylene membrane (Celgard 2400) served as a separator and the electrolyte consisted of 1 M  $\text{LiPF}_6$



in ethylene carbonate/dimethyl carbonate/diethylene carbonate (EC:DMC:DEC, in volumetric ratio of 1:1:1 Targray). The area of the electrode was  $1.77 \text{ cm}^2$ . Firstly, two drops of the electrolyte were applied onto the cathode, then the separator was placed onto the surface of the cathode and the electrolyte was dropped again. Cathodes were prepared using the slurry-casting method as illustrated in **Figure 1**. For that S/DPAN/CNT composite, acetylene black and PVdF were dispersed in N-methyl-2-pyrrolidone (NMP) in the mass ratio of 8:1:1. The prepared slurry was cast as a thin layer on CFP to fill voids using Doctor Blade. The slurry-loaded CFP was cut into two pieces and one was placed on another to obtain a double layered cathode. For a comparison, a thin layer of slurry was cast onto carbon-coated Al foil. Both samples were dried under vacuum at the  $60^\circ\text{C}$  for 12 h. The mass loading of sulfur was about  $1.0 \text{ mg cm}^{-2}$  in the S/DPAN/CNT cathode on the Al foil current collector and about  $3.5\text{--}5 \text{ mg cm}^{-2}$  in cathodes on the double layered CFP. The prepared cells were galvanostatically cycled in a voltage range of 1.0–3.0 V vs.  $\text{Li}^+/\text{Li}$  using the multichannel battery tester (BT-2000, Arbin Instruments Inc.) and the specific capacity was calculated based on the mass of the sulfur in the electrode. A cyclic voltammogram (CV) was received at a potential range from 1 to 3 V vs.  $\text{Li}^+/\text{Li}$  at a scan rate of  $0.1 \text{ mV s}^{-1}$  (VMP3 potentiostat/galvanostat, Bio-Logic Instruments). All the electrochemical measurements were carried out at room temperature.

## RESULTS AND DISCUSSION

Composite cathodes with increased mass loading of sulfur were prepared by simple slurry casting of a S/DPAN/CNT composite on CFP and layering it as shown in **Figure 1**. The slurry-loaded CFPs were layered in a wet condition to increase the amount of sulfur per the unit of electrode area and were dried in a pressed

condition to ensure better contact between layers. The three dimensional structure of the low-weight CFP allowed it to hold a high amount of the S/DPAN/CNT composite, and carbon fibers ensured a high bulk conductivity of the electrode (Suktha et al., 2015). The addition of small amounts of CNT into the composite in the stage of heat treatment improved the electron conduction within the composite spheres.

The morphology of the synthesized S/DPAN/CNT composite was investigated by SEM analysis. **Figure 2A** shows the S/DPAN/CNT composite with 50 wt% sulfur and 3 wt% CNT content which has spherical S/DPAN particles interconnected with CNT. Additionally, the distribution of S, C, and N elements in the composite was analyzed by the SEM/EDS. **Figure 2B** shows the mapping of S, C, and N elements in the S/DPAN/CNT composite, which illustrates the homogenous distribution of sulfur within the composite (**Figure 2B**).

**Figure 3** represents the XRD patterns of the pure components and synthesized composites. It can be seen that CNT shows an intensive peak at about  $27^\circ$ , which can be indexed as the C (002) reflection of the hexagonal graphitic structure, while PAN and sulfur exhibit high crystallinity ( $16.5^\circ$  on PAN and sharp peaks between  $10^\circ$  and  $60^\circ$  S, respectively) (Wang et al., 2015). The XRD patterns of the heat-treated S/DPAN/CNT composite exhibits no peak of crystalline PAN, which was dehydrogenated and probably bound with sulfur during the heat treatment (Chung et al., 2016). The sulfur exhibits two different phase forms according to the XRD analysis which are crystalline and amorphous. The sharp peaks of crystalline sulfur with lower intensity (labelled by star) can still be observed in the S/DPAN/CNT composite with a sulfur content of 54 wt%, while they completely disappeared in the case of the S/DPAN/CNT composite with 50 wt% of sulfur. These sharp peaks are related to the excess sulfur which is not bound with the polymer matrix and remains crystalline on its surface (Wang et al., 2015). The detailed structure information about the S/DPAN composite has

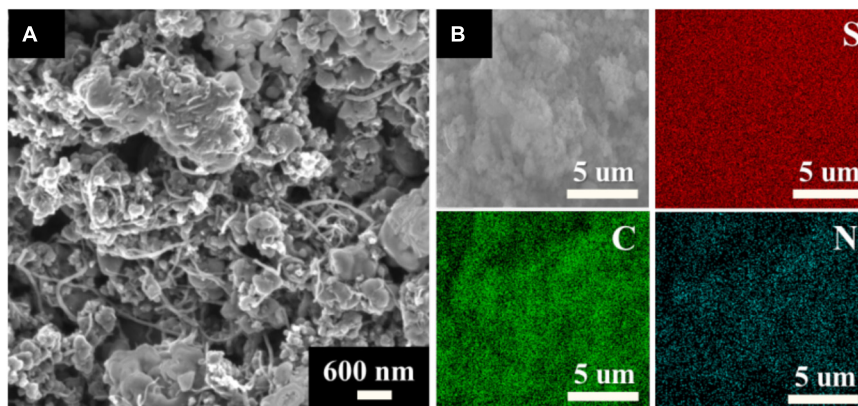


**FIGURE 2** | SEM images of S/DPAN/CNT composite. **(A)** high resolution image of S/DPAN/CNT composite; **(B)** C, S, N element distributions in S/DPAN/CNT composite.

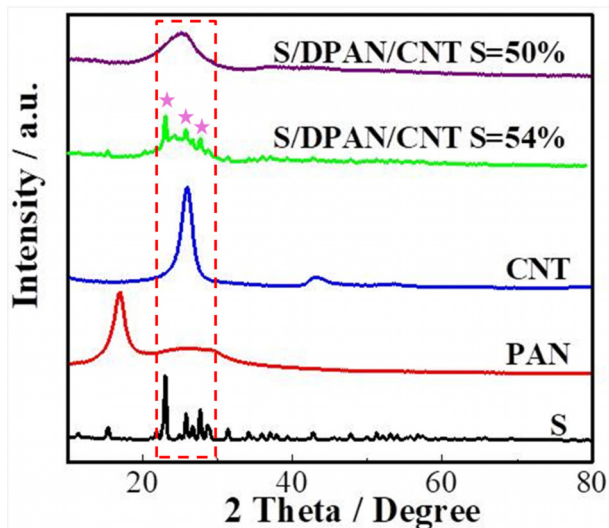


**FIGURE 3** | XRD results of S/DPAN/CNT composites.

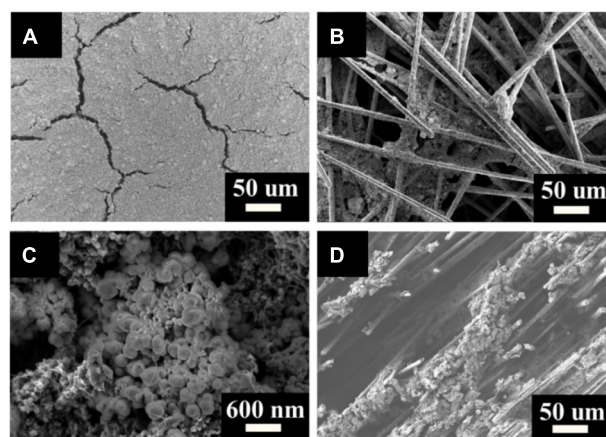


**FIGURE 4** | SEM images of S/DPAN/CNT cathodes. **(A)** S/DPAN/CNT cathode on Al foil, **(B,C)** low and high magnification S/DPAN/CNT cathode on CFP current collector, and **(D)** cross-section view of S/DPAN/CNT cathode on CFP current collector.

been explored and described previously in literature (Wang et al., 2015). Thereby, sulfur bound to the dehydrogenated PAN and converted to an amorphous state, which represents embedding into the heterocyclic structure of PAN (Konarov et al., 2014). Also, the sharp peak of CNT is weakened and overlapped with a broad peak of the amorphous S/DPAN. Therefore, in further experiments S/DPAN/CNT with 50 wt% sulfur was used.

The signals of the C–S and S–S bonds were analyzed by Raman spectra shown in **Supplementary Figure S1**. The elemental sulfur has strong sharp characteristic peaks according to the reports (Yu et al., 2004), which are very weak in the S/DPAN/CNT composite, and some peaks have completely disappeared. The appeared new peaks at 309, 380, 930, and 1149  $\text{cm}^{-1}$  indicate the presence of chemical bonding between cyclized PAN and elemental sulfur (Yu et al., 2004). In the higher frequency region of the Raman spectra (above 1200  $\text{cm}^{-1}$ ), two dominant peaks emerged which

are related to carbon-based materials after pyrolysis of the polymer. The broad peak centered at 1520  $\text{cm}^{-1}$ , often referred as G band, is due to a graphite-like structure, and 1320  $\text{cm}^{-1}$  is due to a disordered structure or D band. The FTIR spectra of the composite was also analyzed to investigate the cyclization of PAN and interaction of sulfur with pyrolyzed PAN (**Supplementary Figure S2**). The FTIR spectrum of PAN has characteristic peaks of –CN and –CH<sub>2</sub> groups at 2244  $\text{cm}^{-1}$  and 1454  $\text{cm}^{-1}$ , while in the spectrum of S/DPAN/CNT several new peaks appeared. The peaks at 1485  $\text{cm}^{-1}$  and 1351  $\text{cm}^{-1}$  correspond to –C = C double bond and –CH deformation, respectively and the peaks at 1413  $\text{cm}^{-1}$  and 800  $\text{cm}^{-1}$  attribute to the cyclized structure of polymer (Kalybekyzy et al., 2019). Moreover, the two new weak peaks detected at 663  $\text{cm}^{-1}$  and 509  $\text{cm}^{-1}$  belong to C–S and S–S stretching vibrations, indicating that sulfur can be chemically bonded with dehydrogenated PAN (DPAN) (Zhang Y.Z. et al., 2014). According to the reports, elemental sulfur is inactive in IR,

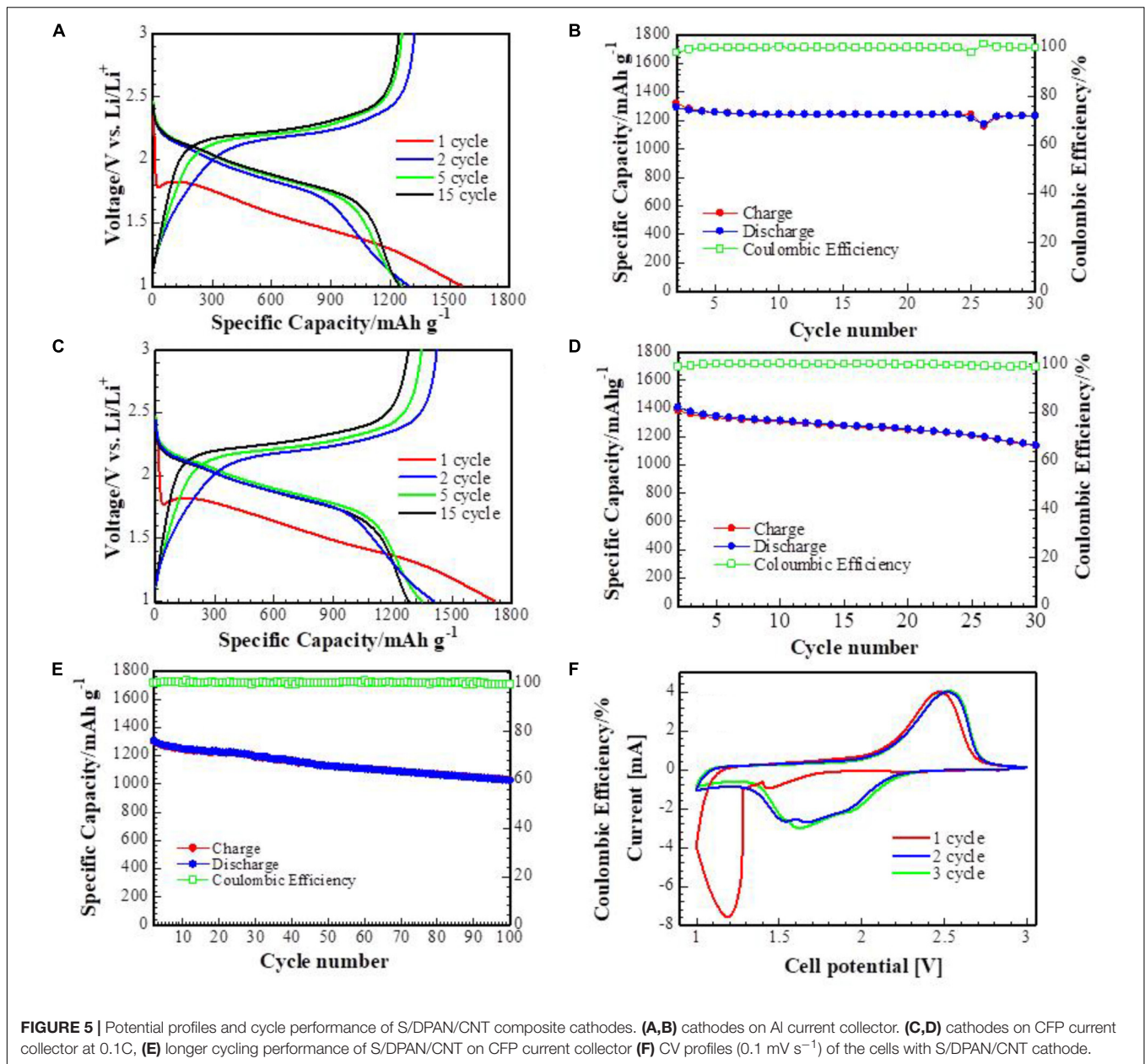


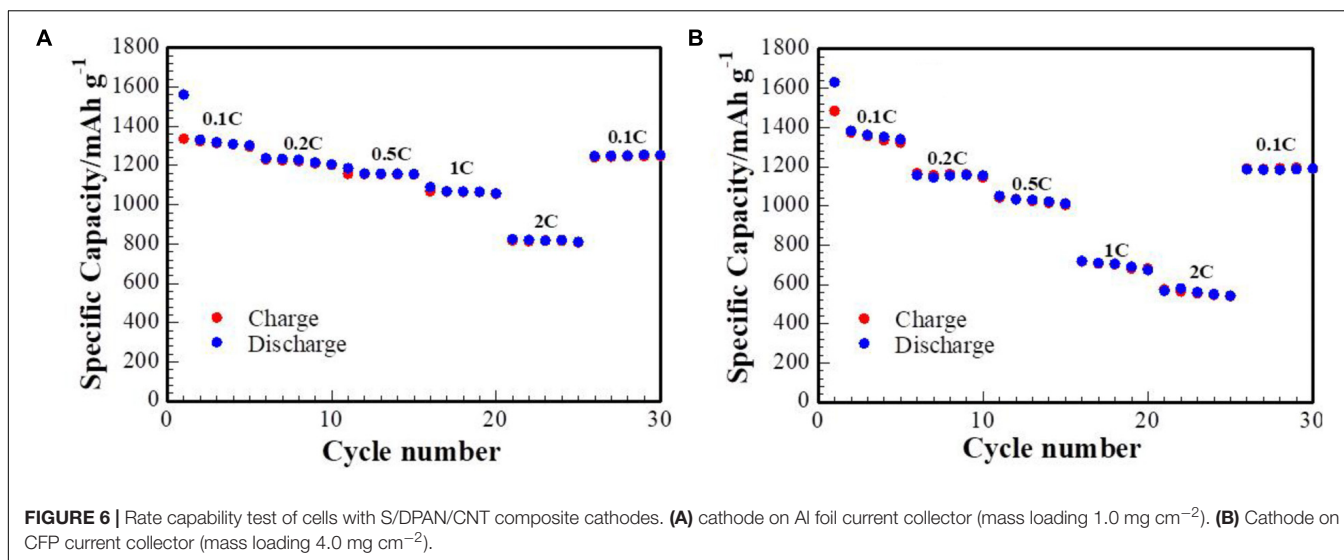
**FIGURE 5** | Potential profiles and cycle performance of S/DPAN/CNT composite cathodes. **(A,B)** cathodes on Al current collector. **(C,D)** cathodes on CFP current collector at 0.1C, **(E)** longer cycling performance of S/DPAN/CNT on CFP current collector **(F)** CV profiles (0.1 mV s<sup>-1</sup>) of the cells with S/DPAN/CNT cathode.

the vibration at 509 cm<sup>-1</sup> can only be caused by the stretching of S–S bonds in the compound-state (Yu et al., 2004). Additionally, the peak at 930 cm<sup>-1</sup> corresponds to the ring breathing in which a C–S bond is also included together with the side chain of the S–S ring (Wang et al., 2012; Chen et al., 2019). Therefore, these characteristic peaks verify the structure of C–S and S–S bonds after the dehydrogenation reaction.

The morphology of the S/DPAN/CNT cathodes on Al foil and CFP was analyzed by SEM as shown in Figure 4. The SEM image of the S/DPAN/CNT composite cathode on an Al foil current collector (Figure 4A), indicate that the slurry was homogeneously distributed onto the surface of the current collector, while cracks of 7 μm in width appeared on its surface due to solvent evaporation. In the case of the CFP current

collector (Figures 4B,C), the main part of the composite cathode was loaded into the large free space between interconnected carbon fibers. Moreover, the complete filling of the free space between the layers of CFP can be confirmed by the cross-section SEM image (Figure 4D). A SEM image with higher magnification (Figure 4C) shows that hundreds of nanometers in size particles of S/DPAN are bridged with CNTs and the small particles of a conductive agent (AB, 10 wt%). Also, mapping of the elements in the S/DPAN/CNT composite cathode on CFP illustrates the homogenous distribution of S, C, and N elements within the electrode (Supplementary Figure S3).

Electrochemical performance of the S/DPAN/CNT composite cathode with different amounts of CNT (1–4%) was tested using a carbon coated Al foil current collector



(**Supplementary Figure S4**) with an equal sulfur content (50%) and mass loading of  $1.0 \text{ mg cm}^{-2}$ . The S/DPAN/CNT composite cathode with 3% CNT showed the highest capacity retention and lower polarization among other composite cathodes. However, increasing the amount of CNT up to 4% shows no improvement in electrochemical performance. Comparative analysis of the EIS data was performed on the electrodes with equal mass loading of sulfur of  $1.0 \text{ mg cm}^{-2}$  (**Supplementary Figure S5**). Increasing the content of CNT led to a smaller charge transfer resistance which could refer to the conductivity improvement due to the addition of highly conductive CNT (Mentbayeva et al., 2016; Li T. et al., 2017). Therefore, the S/DPAN/CNT composite cathode with 3 wt% CNT was used in further experiments.

**Figures 5A–E** represent galvanostatic charge-discharge and cyclability of Li-S cells with the S/DPAN/CNT with 3 wt% CNT composite cathode on the Al and CFP current collectors. The composite cathode on Al foil with sulfur mass loading of  $1 \text{ mg cm}^{-2}$  delivers a high discharge capacity of  $1350 \text{ mAh g}^{-1}$  at the 2nd cycle at 0.1C. At the first 30 cycles the cells performed stable capacity retention with a high coulombic efficiency of about 100%. At the same time the cathode on the CFP current collector showed similar specific capacity at the 2nd, 5th, and 15th cycles when the mass loading of sulfur was increased up to  $5 \text{ mg cm}^{-2}$ . Similar electrochemical results of the composite cathode on CFP compared to the cathode on the Al foil can be explained in terms of the high conductivity of long carbon fibers (Suktha et al., 2015), which ensures the electrode integrity while large voids of CFP provides mechanical support to accommodate volume change, and CNT maintains structural integrity and faster electron conduction at the micro level (Peng et al., 2017b; Qin et al., 2017). The longer cycling performance of the cell with the S/DPAN/CNT composite cathode on the CFP current collector and sulfur mass loading of  $4 \text{ mg cm}^{-2}$  is illustrated in **Figure 5E**. It can be seen that the cell maintained a stable capacity of  $1030 \text{ mAh g}^{-1}$  at the 100th cycle.

**Figure 5F** illustrates CV curves of the cathode on the CFP current collector. The composite cathode exhibits a large reduction peak at  $1.2 \text{ V vs. Li}^+/\text{Li}$ . This peak slightly moves to the higher voltage at the next cycle. A large polarization between the reduction and oxidation peaks during the first cycles could stem from the generation of the solid electrolyte interface (SEI) on the anode surface (Zhang et al., 2013). During the following cycles a large oxidation peak at  $2.5 \text{ V vs. Li}^+/\text{Li}$  and two reduction peaks at  $1.7$  and  $1.6 \text{ V}$  presented, which can be explained by the formation of long-chain lithium polysulfides and low-order lithium sulfides (Zhang et al., 2013).

**Figure 6** represents the rate step-progressive test of batteries with S/DPAN/CNT (3 wt% CNT) composite cathodes on both Al foil and CFP current collectors, where cells were galvanostatically cycled at current densities ranging from 0.1C up to 2C. At the lower current densities of 0.1C, 0.2C, 0.5C, and 1C stable capacities of  $1340$ ,  $1215$ ,  $1160$ ,  $1050 \text{ mAh g}^{-1}$ , respectively, were achieved, while the 2C capacity of  $791 \text{ mAh g}^{-1}$  was obtained for the cathode on the Al foil current collector. Then the initial capacity of  $1245 \text{ mAh g}^{-1}$  was regenerated when the current density was lowered back to 0.1C. In comparison, the cathode on the CFP current collector with mass loading of sulfur at  $4.0 \text{ mg cm}^{-2}$  showed stable capacities of  $1345$ ,  $1150$ ,  $1010$ ,  $650$ ,  $570 \text{ mAh g}^{-1}$ , respectively. High capacity retention can be observed when the current density was lowered back to 0.1C. Thus, the CFP fibers provide better conductivity and better active material utilization was achieved at high cycling rates.

Increasing the mass loading of sulfur should go along with the addition of conductive agents in order to provide sufficient bulk conductivity. As described above the addition of 3% CNT significantly lowers the charge transfer resistance (**Supplementary Figure S5**). Consequently, the entrapping of composite cathodes into a 3D structured CFP current collector and the addition of small amounts of CNT to the composite

remarkably improves the electron conduction of the cathode, which enables a reasonable C rate performance of the cathode with mass loading as high as  $4 \text{ mg cm}^{-2}$ .

The post-cycling morphology of the S/DPAN/CNT composite cathode on the CFP current collector after 30 cycles of discharge and charge processes was analyzed using SEM (**Supplementary Figure S6**). A SEM image with high magnification clearly shows the agglomeration of the particles, which can be explained by the irreversible formation of low order lithium sulfides due to the partial loss of contact between the composite cathode and current collector (Pan et al., 2015). This is one of the reasons of the capacity decay of the cell upon cycling. In general, there are minor changes in surface morphology. Particles are equally distributed between long carbon fibers, which can be explained by the strong adhesion and stability of the composite.

## CONCLUSION

To sum up, a S/DPAN/CNT composite cathode with 1–4% CNT and 50 wt% sulfur content was synthesized by manual mixing of sulfur, PAN, and CNT followed by heating in an argon atmosphere. Composites with 3 wt% CNT showed better electrochemical performance among other composites (1–4 wt% CNT). The results of both Raman and FTIR spectra of the composite showed the interaction of sulfur with PAN (S-C bond) and cyclization of PAN. Fixing sulfur to a pyrolyzed PAN structure can diminish the dissolution of polysulfides, while CNT acts as interwoven network and maintains structural integrity. Injection of S/DPAN/CNT into double layered CFP allowed for obtaining a high mass loading ( $5.0 \text{ mg cm}^{-2}$ ) sulfur composite cathode with initial capacity of  $1400 \text{ mAh g}^{-1}$ . The cells with a mass loading of sulfur of  $4 \text{ mg cm}^{-2}$  showed stable capacity retention up to 100 cycles and a stable rate capability, due to improved bulk conductivity of the cathode by carbon fibers and CNT.

## REFERENCES

- Bakenov, Z., Yashiro, H., Sun, Y.-K., Myung, S.-T., and Konarov, A. (2017). Effect of carbon-sulphur bond in a sulphur/dehydrogenated polyacrylonitrile/reduced graphene oxide composite cathode for lithium-sulphur batteries. *J. Power Sources* 355, 140–146. doi: 10.1016/j.jpowsour.2017.04.063
- Chen, X., Peng, L., Wang, L., Yang, J., Hao, Z., Xiang, J., et al. (2019). Ether-compatible sulfurized polyacrylonitrile cathode with excellent performance enabled by fast kinetics via selenium doping. *Nat. Commun.* 10, 1–9. doi: 10.1038/s41467-019-08818-6
- Cheng, X.-B., Huang, J.-Q., Zhang, Q., Xu, W.-T., Peng, H.-J., Wang, D.-W., et al. (2016). 3D carbonaceous current collectors: the origin of enhanced cycling stability for high-sulfur-loading lithium-sulfur batteries. *Adv. Funct. Mater.* 26, 6351–6358. doi: 10.1002/adfm.201602071
- Chung, S. H., Chang, C. H., and Manthiram, A. (2016). A carbon-cotton cathode with ultrahigh-loading capability for statically and dynamically stable lithium-sulfur batteries. *ACS Nano* 10, 10462–10470. doi: 10.1021/acsnano.6b06369
- Chung, S. H., and Manthiram, A. (2018). Rational design of statically and dynamically stable lithium-sulfur batteries with high sulfur loading and low electrolyte/sulfur ratio. *Adv. Mater.* 30, 1–9. doi: 10.1002/adma.201705951

## DATA AVAILABILITY STATEMENT

All datasets presented in this study are included in the article/**Supplementary Material**.

## AUTHOR CONTRIBUTIONS

AM: conceptualization, methodology, validation, data curation, writing – original draft, and supervision. NB: writing – original draft, data curation, and writing – review and editing. NS: validation, investigation, and visualization. SK: investigation, recourses, and visualization. IK: investigation and recourses. ZB: writing – review and editing, and funding acquisition.

## FUNDING

This work was supported by the Faculty development competitive research grant #080420FD1906 from Nazarbayev University and by the State Target Program #BR05236524 from the Ministry of Education and Science of the Republic of Kazakhstan.

## ACKNOWLEDGMENTS

The authors thank the Shared Facility of Nazarbayev University for access to laboratory equipment.

## SUPPLEMENTARY MATERIAL

The Supplementary Material for this article can be found online at: <https://www.frontiersin.org/articles/10.3389/fenrg.2020.00207/full#supplementary-material>

- Guo, J., Xu, Y., and Wang, C. (2011). Sulfur-impregnated disordered carbon nanotubes cathode for lithium-sulfur batteries. *Nano Lett.* 11, 4288–4294. doi: 10.1021/nl202297p
- Hara, T., Konarov, A., Mentbayeva, A., Kurmanbayeva, I., and Bakenov, Z. (2015). High mass-loading of sulfur-based cathode composites and polysulfides stabilization for rechargeable lithium/sulfur batteries. *Front. Energy Res.* 3:22. doi: 10.3389/fenrg.2015.00022
- Kalybekkyzy, S., Mentbayeva, A., Kahraman, M. V., Zhang, Y., and Bakenov, Z. (2019). Flexible S/DPAN/KB Nanofiber Composite as Binder-Free Cathodes for Li-S Batteries. *J. Electrochem. Soc.* 166, A5396–A5402. doi: 10.1149/2.0571903jes
- Kalybekkyzy, S., Mentbayeva, A., Yerkinbekova, Y., Baikalov, N., Kahraman, M. V., and Bakenov, Z. (2020). Electrospun 3D structured carbon current collector for Li/S batteries. *Nanomaterials* 10, 1–13. doi: 10.3390/nano10040745
- Konarov, A., Gosselink, D., Doan, T. N. L., Zhang, Y., Zhao, Y., and Chen, P. (2014). Simple, scalable, and economical preparation of sulfur-PAN composite cathodes for Li/S batteries. *J. Power Sources* 259, 183–187. doi: 10.1016/j.jpowsour.2014.02.078
- Li, G., Wang, S., Zhang, Y., Li, M., Chen, Z., and Lu, J. (2018). Revisiting the Role of Polysulfides in Lithium-sulfur batteries. *Adv. Mater.* 30, 1–19. doi: 10.1002/adma.201705590
- Li, H., Wang, J., Zhang, Y., Wang, Y., Mentbayeva, A., and Bakenov, Z. (2019). Synthesis of carbon coated Fe<sub>3</sub>O<sub>4</sub> grown on graphene as effective sulfur-host

- materials for advanced lithium/sulfur battery. *J. Power Sources* 437, 226901. doi: 10.1016/j.jpowsour.2019.226901
- Li, M., Carter, R., Douglas, A., Oakes, L., and Pint, C. L. (2017). Sulfur Vapor-Infiltrated 3D Carbon Nanotube foam for binder-free high areal capacity Lithium-Sulfur battery composite cathodes. *ACS Nano* 11, 4877–4884. doi: 10.1021/acsnano.7b01437
- Li, T., Bo, H., Cao, H., Lai, Y., Liu, Y., and Huang, Z. (2017). Effects of carbon hosts on electrochemical properties of lithium-sulfur batteries. *Int. J. Electrochem. Sci.* 12, 5731–5741. doi: 10.20964/2017.06.41
- Lu, S., Chen, Y., Wu, X., Wang, Z., and Li, Y. (2014). Three-dimensional sulfur/graphene multifunctional hybrid sponges for lithium-sulfur batteries with large areal mass loading. *Sci. Rep.* 4, 4–7. doi: 10.1038/srep04629
- Ma, W., and Xu, Q. (2018). Lithium cobaltate: a novel host material enables high-rate and stable lithium-sulfur batteries. *Rare Met.* 37, 929–935. doi: 10.1007/s12598-018-1129-4
- Mentbayeva, A., Belgibayeva, A., Umirov, N., Zhang, Y., Taniguchi, I., Kurmanbayeva, L., et al. (2016). High performance freestanding composite cathode for lithium-sulfur batteries. *Electrochim. Acta* 217, 242–248. doi: 10.1016/j.electacta.2016.09.082
- Nie, Z., Zhang, J.-G., Browning, N. D., Li, Q., Mehdi, L. B., Xie, X., et al. (2015). High energy density Lithium-Sulfur Batteries: challenges of thick Sulfur Cathodes. *Adv. Energy Mater.* 5:1402290. doi: 10.1002/aenm.201402290
- Ould Ely, T., Kamzabek, D., Chakraborty, D., and Doherty, M. F. (2018). Lithium-Sulfur batteries: state of the art and future directions. *ACS Appl. Energy Mater.* 1, 1783–1814. doi: 10.1021/acsaem.7b00153
- Pan, J., Xu, G., Ding, B., Han, J., Dou, H., and Zhang, X. (2015). Enhanced electrochemical performance of sulfur cathodes with a water-soluble binder. *RSC Adv.* 5, 13709–13714. doi: 10.1039/c4ra15303k
- Peng, H., Huang, J., Cheng, X., and Zhang, Q. (2017a). Review on high-loading and high-energy Lithium – Sulfur Batteries. 1700260, 1–54. doi: 10.1002/aenm.201700260
- Peng, H., Wang, X., Zhao, Y., Tan, T., Mentbayeva, A., Bakenov, Z., et al. (2017b). Enhanced electrochemical performance of sulfur/polyacrylonitrile composite by carbon coating for lithium/sulfur batteries. *J. Nanoparticle Res.* 19:348. doi: 10.1007/s11051-017-4049-6
- Peng, H., Wang, X., Zhao, Y., Tan, T., Bakenov, Z., and Zhang, Y. (2018). Synthesis of a flexible freestanding sulfur/polyacrylonitrile/graphene oxide as the cathode for lithium/sulfur batteries. *Polymers* 10, 1–10. doi: 10.3390/polym10040399
- Qin, F., Wang, X., Zhang, K., Fang, J., Li, J., and Lai, Y. (2017). High areal capacity cathode and electrolyte reservoir render practical Li-S batteries. *Nano Energy* 38, 137–146. doi: 10.1016/j.nanoen.2017.05.037
- Rajkumar, P., Diwakar, K., Subadevi, R., Gnanamuthu, R. M., and Sivakumar, M. (2019). Sulfur cloaked with different carbonaceous materials for high performance lithium sulfur batteries. *Curr. Appl. Phys.* 19, 902–909. doi: 10.1016/j.cap.2019.05.001
- Shin, K.-H., Kim, K.-B., Jin, C.-S., Ahn, W., and Jung, K.-N. (2011). Synthesis and electrochemical properties of a sulfur-multi walled carbon nanotubes composite as a cathode material for lithium sulfur batteries. *J. Power Sources* 202, 394–399. doi: 10.1016/j.jpowsour.2011.11.074
- Song, X., Wang, S., Bao, Y., Liu, G., Sun, W., Ding, L. X., et al. (2017). A high strength, free-standing cathode constructed by regulating graphitization and the pore structure in nitrogen-doped carbon nanofibers for flexible lithium-sulfur batteries. *J. Mater. Chem. A* 5, 6832–6839. doi: 10.1039/C7TA01171G
- Suktha, P., Chiochan, P., Iamprasertkun, P., Wuthiprom, J., Phattharasupakun, N., Suksomboon, M., et al. (2015). High-Performance Supercapacitor of Functionalized Carbon Fiber Paper with High Surface ionic and bulk electronic conductivity: effect of organic functional groups. *Electrochim. Acta* 176, 504–513. doi: 10.1016/j.electacta.2015.07.044
- Wang, B. J., Yang, J., Wan, C., Du, K., Xie, J., and Xu, N. (2003). Sulfur Composite Cathode Materials for Rechargeable Lithium Batteries. *Adv. Funct. Mater.* 13, 487–492. doi: 10.1002/adfm.200304284
- Wang, J., He, Y. S., and Yang, J. (2015). Sulfur-based composite cathode materials for high-energy rechargeable lithium batteries. *Adv. Mater.* 27, 569–575. doi: 10.1002/adma.201402569
- Wang, L., He, X., Li, J., Gao, J., Guo, J., Jiang, C., et al. (2012). Analysis of the synthesis process of sulphur-poly(acrylonitrile)-based cathode materials for lithium batteries. *J. Mater. Chem.* 22, 22077–22081. doi: 10.1039/c2jm30632h
- Yang, C. P., Yin, Y. X., Ye, H., Jiang, K. C., Zhang, J., and Guo, Y. G. (2014). Insight into the effect of boron doping on sulfur/carbon cathode in lithium-sulfur batteries. *ACS Appl. Mater. Interfaces* 6, 8789–8795. doi: 10.1021/am501627f
- Ye, X., Ma, J., Hu, Y. S., Wei, H., and Ye, F. (2016). MWCNT porous microspheres with an efficient 3D conductive network for high performance lithium-sulfur batteries. *J. Mater. Chem. A* 4, 775–780. doi: 10.1039/c5ta08991c
- Yin, L., Wang, J., Lin, F., Yang, J., and Nuli, Y. (2012). Polyacrylonitrile/graphene composite as a precursor to a sulfur-based cathode material for high-rate rechargeable Li-S batteries. *Energy Environ. Sci.* 5, 6966–6972. doi: 10.1039/c2ee03495f
- Yu, X., Deng, J., Lv, R., Huang, Z. H., Li, B., and Kang, F. (2018). A compact 3D interconnected sulfur cathode for high-energy, high-power and long-life lithium-sulfur batteries. *Energy Storage Mater.* 20, 1–10. doi: 10.1016/j.enstm.2018.11.029
- Yu, X. G., Xie, J. Y., Yang, J., Huang, H. J., Wang, K., and Wen, Z. S. (2004). Lithium storage in conductive sulfur-containing polymers. *J. Electroanal. Chem.* 573, 121–128. doi: 10.1016/j.jelechem.2004.07.004
- Yuan, L., Yuan, H., Qiu, X., Chen, L., and Zhu, W. (2009). Improvement of cycle property of sulfur-coated multi-walled carbon nanotubes composite cathode for lithium/sulfur batteries. *J. Power Sources* 189, 1141–1146. doi: 10.1016/j.jpowsour.2008.12.149
- Zeng, F., Wang, W., Wang, A., Yuan, K., Jin, Z., and Yang, Y. (2015). Multidimensional Polycation  $\beta$  - Cyclodextrin Polymer as an Effective Aqueous Binder for High Sulfur Loading Cathode in Lithium – Sulfur Batteries. *ACS Appl. Mater. Interfaces* 7, 26257–26265. doi: 10.1021/acsmi.5b08537
- Zhang, Y., Bakenov, Z., Zhao, Y., Konarov, A., Doan, T. N. L., Malik, M., et al. (2012). One-step synthesis of branched sulfur/polypyrrole nanocomposite cathode for lithium rechargeable batteries. *J. Power Sources* 208, 1–8. doi: 10.1016/j.jpowsour.2012.02.006
- Zhang, Y., Zhao, Y., Yermukhambetova, A., Bakenov, Z., and Chen, P. (2013). Ternary sulfur/polyacrylonitrile/Mg<sub>0.6</sub>Ni<sub>0.4</sub>O composite cathodes for high performance lithium/sulfur batteries. *J. Mater. Chem. A* 1, 295–301. doi: 10.1039/c2ta00105e
- Zhang, Y. Z., Liu, S., Li, G. C., Li, G. R., and Gao, X. P. (2014). Sulfur/polyacrylonitrile/carbon multi-composites as cathode materials for lithium/sulfur battery in the concentrated electrolyte. *J. Mater. Chem. A* 2, 4652–4659. doi: 10.1039/c3ta14914e
- Zhang, Y., Zhao, Y., Bakenov, Z., Tuiyebayeva, M., Konarov, A., and Chen, P. (2014). Synthesis of hierarchical porous sulfur/polypyrrole/multiwalled carbon nanotube composite cathode for lithium batteries. *Electrochim. Acta* 143, 49–55. doi: 10.1016/j.electacta.2014.07.148
- Zhao, Y., Zhang, Y., Bakenova, Z., and Bakenov, Z. (2015). Carbon/Sulfur Composite Cathodes for Flexible Lithium/Sulfur batteries: status and prospects. *Front. Energy Res.* 3:2. doi: 10.3389/fenrg.2015.00002

**Conflict of Interest:** ZB and IK were employed by the company Institute of Batteries LLC.

The remaining authors declare that the research was conducted in the absence of any commercial or financial relationships that could be construed as a potential conflict of interest.

Copyright © 2020 Baikarov, Serik, Kalybekkyzy, Kurmanbayeva, Bakenov and Mentbayeva. This is an open-access article distributed under the terms of the Creative Commons Attribution License (CC BY). The use, distribution or reproduction in other forums is permitted, provided the original author(s) and the copyright owner(s) are credited and that the original publication in this journal is cited, in accordance with accepted academic practice. No use, distribution or reproduction is permitted which does not comply with these terms.